Polymer Journal, Vol. 12, No. 3, pp 161—170 (1980)

Solution Properties of Synthetic Polypeptides. XXII. Helix–Coil Transition of Poly(N^{γ}-carbobenzoxy-L-α,γ-diaminobutyric acid)

Sigeru SARUTA, Yoshiyuki EINAGA, and Akio TERAMOTO

Department of Polymer Science, Osaka University, Toyonaka, Osaka 560, Japan.

(Received October 23, 1979)

ABSTRACT: The helix–coil transition of poly(N^{γ}-carbobenzoxy-L-α,γ-diaminobutyric acid) (PCLB) in mixtures of dichloroacetic acid (DCA) and 1,2-dichloroethane (EDC) was studied by optical rotatory dispersion (ORD) measurement. At DCA contents between 55 and 58 vol%, the Moffitt parameter b_0 increased with increasing temperature, passed through a maximum, and gradually decreased above 40°C. This result indicates that in mixtures of DCA and EDC of appropriate compositions, PCLB undergoes a dual transition: one which is normal (helix to coil) at lower temperatures and one which is inverse (coil to helix) at higher temperatures. The ORD data were analyzed theoretically to evaluate the equilibrium constant s for the helix formation as a function of temperature T and solvent composition. A plot of ln s at a fixed solvent composition against $1/T$ followed a curve convex downward, corresponding to the dual transition. The conformation of PCLB in a helicogenic solvent, dimethyl sulfoxide, was investigated by light scattering and viscometry, and it was found from the observed relation between the mean-square radius of gyration $\langle S^2 \rangle$ and molecular weight that PCLB takes on the form of an interrupted helix in this solvent. The molecular weight dependence of $\langle S^2 \rangle$ and intrinsic viscosity indicates that the helix of PCLB is as stable as those of poly(N^{ε}-carbobenzoxy-L-lysine) and poly(N^{δ}-carbobenzoxy-L-ornithine), but less stable than that of poly(γ-benzyl L-glutamate).

KEY WORDS Poly(N^{γ}-carbobenzoxy-L-α,γ-diaminobutyric acid) / Helix–Coil Transition / α-Helix / Transition Enthalpy / Interrupted Helix / Light Scattering / Mean-Square Radius of Gyration / Particle Scattering Function / Intrinsic Viscosity /

The helix–coil transition of a nonionic polypeptide in solution is caused either by changing the temperature in a fixed solvent or by changing the composition of a binary mixture composed of a helix-breaking solvent such as dichloroacetic acid (DCA) and a helix-supporting solvent such as 1,2-dichloroethane (EDC).[1-4] The stability of a helical conformation and the feature of helix–coil transition depend markedly on the side chain attached to the α-carbon atom.[1-4] To make an experimental study of this dependence, we have chosen a family of synthetic polypeptides shown below.

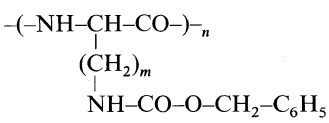

Here the polypeptides for $m=2$, 3, and 4 are poly(N^{γ}-carbobenzoxyl-L-α,γ-diaminobutyric acid) (PCLB), poly(N^{δ}-carbobenzoxyl-L-ornithine) (PCLO), and poly(N^{ε}-carbobenzoxy-L-lysine) (PCBL), respectively. Gaskin and Yang[5] found that PCLB underwent a normal helix–coil transition in a mixture of DCA and chloroform, whereas PCLO exhibited an inverse helix–coil transition in the same solvent system. It is rather surprising that a change in only one methylene group of the side chain reverses the direction of the thermal transition.

It is usually considered that the direction of thermal transition is determined by two competitive actions. One of these is the formation of intramolecular hydrogen bonds between pairs of peptide residues of the polypeptide backbone. This action promote the helix formation, and its strength

is a measure of the intrinsic stability of the polypeptide helix. The other action is that of the hydrogen bond formation between an acidic liquid such as DCA and the polypeptide main chain and disrupts helical conformation. The former action induces a normal transition, whereas the latter induces an inverse transition. Statistical mechanical theories of the helix–coil transition of polypeptide have been developed, taking these actions into consideration, and prediction based on these theories has been tested thoroughly with experimental data.[4] The major prediction is that an inverse transition should be followed by a normal transition at high temperatures when the solvent is a mixture of a helix-breaking liquid and a helix-supporting liquid.[4,6] It is interesting to examine whether or not the normal transition of PCLB as found by Gaskin and Yang fits to this theoretical prediction.

The purpose of the present paper is twofold: first, to obtain experimental data for the helix–coil transition of PCLB in mixtures of DCA and EDC over a wider range of temperature and solvent composition than in the study of Gaskin and Yang, and second, to estimate the stability of the helical conformation of this polypeptide from light scattering and viscosity data in helix-supporting solvents.

EXPERIMENTAL

Polypeptide Samples

N^{γ}-Carbobenzoxy L-α,γ-diaminobutyric acid N-carboxy anhydride (CLB-NCA) was synthesized from L-glutamic acid, following the route illustrated below.

L-glutamic acid $\xrightarrow{A}$ L-α,γ-diaminobutyric acid dihydrochloride $\xrightarrow{B}$ N^{γ}-carbobenzoxy-L-α,γ-diaminobutyric acid (CLB) $\xrightarrow{C}$ CLB-NCA

Adamson's method[7] was employed for process A. Reactions B and C were carried out according to the method of Fridecky and McGregor.[8] L-Glutamic acid (Ajinomoto K.K.) was used as received. All other chemicals used were of reagent grade. The synthesized CLB-NCA was recrystallized several times from a mixture of ethyl acetate, chloroform, and hexane, and stored at −20°C.

The CLB-NCA was allowed to polymerize in a mixture of dioxane and *N,N*-dimethylformamide (DMF) with triethylamine as the initiator. After standing for 24 h with stirring, the reaction mixture was poured into a large volume of methanol, and the precipitated PCLB was collected on a sintered-glass filter, washed with methanol, and dried *in vacuo*. The molecular weights of the samples showed hardly any change according to the solvent composition, the concentration of NCA, or the molar ratio of NCA to initiator but depended on the purities of the NCA preparation and the solvent used.

Samples with similar intrinsic viscosities in *m*-cresol at 25°C were combined and separated into several fractions by fractional precipitation, with DMF as the solvent and methanol as the precipitant. Those fractions with similar intrinsic viscosities were recombined and fractionated again by a similar procedure. The final fractions were repeatedly purified by dissolving in DMF and precipitating into methanol. Seven fractions were selected from these for physical measurements.

PCLB was found to dissolve in DCA, dimethylsulfoxide (DMSO), hexamethylphosphoramide, *N*-methyl-2-pyrrolidone, trimethylphosphate, and tetramethylurea. Fresh PCLB was soluble in DMF, but became insoluble after storage. Samples with molecular weights smaller than 10^5 dissolved in EDC, chloroform, and dichloromethane.

Light Scattering and Osmotic Pressure

Light scattering measurements were made in DMSO at 25°C, using a Fica 50 automatic light scattering photogoniometer with cylindrical glass cells. The experimental procedure and the method for data analysis were essentially the same as those described elsewhere.[9] Test solutions and solvent were centrifuged at 40,000 g for 4—7 h and directly pipetted into the cells. Data were taken at scattering angles between 30° and 150°, with a vertically polarized incident light of wavelength 436 nm.

The data were analyzed by means of Berry's square-root method to evaluate the weight-average molecular weight M_w, the mean (−) square radius of gyration $\langle S^2 \rangle$, and the second virial coefficient A_2'. A differential refractometer of the modified Schulz–Cantow type was used for measuring the specific refractive index increment $\partial n/\partial c$ of PCLB in DMSO.

The values of $\partial n/\partial c$ for wavelengths of 436 nm and 546 nm at 25°C were 0.087_2 cm^3 g^{-1} and 0.083_1 cm^3 g^{-1}, respectively.

The osmotic pressures of *m*-cresol solutions at 70°C were measured by using a Knauer membrane osmometer with a Sartorius membrane filter SM-11536 carefully conditioned.

Results from the light scattering and osmotic pressure measurements are summarized in Table I. Here, M_n is the number-average molecular weight and A_2 is the osmotic second virial coefficient. The polydispersity index M_w/M_n scatters between 1.36 and 1.85. These numbers indicate that the fractionated samples were rather polydisperse in molecular weight.

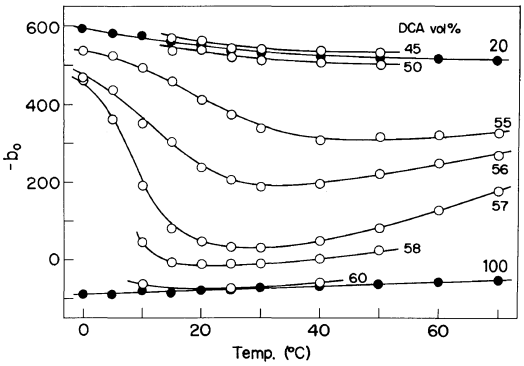

Figure 1. Plots of Moffitt parameter b_0 *vs.* temperature for the sample T-1 in DCA–EDC mixtures. The composition of each solvent mixture is indicated by vol% DCA at 25°C.

Viscometry

Viscosities were measured by capillary viscometers of the Ubbelohde type with negligible kinetic energy correction. Data were taken at 25°C in DMSO, *m*-cresol, and DCA containing various amounts of lithium chloride.

Optical Rotatory Dispersion

Optical rotatory dispersion curves were obtained in DCA–EDC mixtures of various compositions, in a DCA–chloroform mixture at various temperatures between 0°C and 70°C, and in DMSO at 25°C. A JASCO Model ORD–UV-5 recording spectropolarimeter with quartz cells of 10 cm path lengths was used. Data were taken at wavelengths ranging from 300 to 600 nm and analyzed by the Moffitt–Yang equation to determine the Moffitt parameter b_0, with λ_0 taken as 212 nm. Solvent mixtures and polypeptide solutions were prepared gravimetrically. DCA, DMSO, and *m*-cresol were distilled under reduced nitrogen atmosphere after drying over sulfuric acid for DCA, calcium oxide for DMSO, and phosphorous pentoxide for *m*-cresol. These solvents were used immediately after distillation, and all manipulations involving them were performed under a dry nitrogen atmosphere. The other organic liquids used were purified by the standard procedure.[10]

RESULTS AND DISCUSSION

Helix–Coil Transition

Figure 1 shows the dependence of the Moffitt parameter b_0 on the solvent composition and temperature for a high-molecular-weight sample of PCLB in DCA–EDC mixtures. For the solvent mixtures containing 50 vol% or less DCA, the values of $(-)$ b_0 are about 500 and decrease gradually with rise in temperature; the maximum value of $-b_0$ is 595 in the 45 vol% DCA at 10°C. The b_0 values in the solvent mixtures containing 45 vol% or less DCA were nearly independent of solvent composition and molecular weight. We conclude from these results that the molecular conformation of PCLB is essentially α-helical under these solvent conditions, since the b_0 for helical L-polypeptides are usually in the range between -500 and -700[1,2] and theoretically b_0 should not depend on molecular weight provided the conformation is perfectly helical. Hence, we took the b_0 values for sample T-1 in a DCA–EDC mixture (20 vol% DCA) as those for a perfect helix. The b_0 values in pure DCA and in a DCA–EDC mixture of 60 vol% DCA were about 60 in the temperature range examined and depended only slightly on molecular weight. Thus we conclude that PCLB assumes a random coil under these solvent conditions. At 57 vol% DCA, the value of $-b_0$ decreases rather sharply in the region below 20°C, passes through a minimum, and then swings up, as the temperature is raised. With the understanding that b_0 is linearly related to the helical fraction f_N, we may conclude that PCLB in mixtures of DCA and EDC undergoes a normal transition at low temperatures and an inverse transition at higher temperatures. PCLB is the only polypeptide known to undergo this type of helix–coil transition.

Figure 2 shows a plot of b_0 *vs.* temperature for

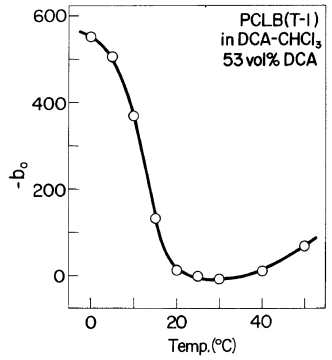

Figure 2. Temperature dependence of Moffitt parameter b_0 for the sample T-1 in a DCA–$CHCl_3$ (53 vol% DCA) mixture.

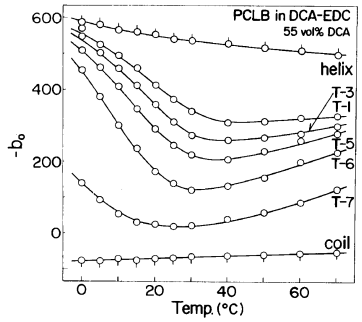

Figure 3. Temperature dependence of Moffitt parameter b_0 for PCLB in a DCA–EDC (55 vol% DCA) mixture as a function of molecular weight. Circles with pip up and pip down represent b_0 values for perfect helix and perfect random coil, respectively.

sample T-1 in chloroform containing 53 vol% DCA. We can see that PCLB undergoes a dual thermal transition similar to those observed in DCA–EDC mixtures. The normal transition in these solvent mixtures at low temperature confirms the finding of Gaskin and Yang[5] and of Giacometti *et al.*[11], but neither of these authors noticed that this transition would be followed by an inverse transition at higher temperatures.

Figure 3 shows the effect of molecular weight on the helix–coil transition of PCLB in a DCA–EDC mixture (55 vol% DCA). Here the molecular weights of the samples decrease in order from T-1 to T-7 (see Table I). The curves "helix" and "coil" refer to the b_0 values for a perfect helix and random coil, respectively. In the discussion that follows, all b_0 data are converted to the helical fraction f_N, assuming a linear relation between f_N and b_0 with the limiting b_0 values given above. For any of the samples studied, the helical fraction first decreases rather sharply in the region below 30—40°C and then increases gradually, as the temperature is raised. The position of the minimum in the transition curve shifts to lower temperature and lower f_N as the molecular weight is decreased. As the theories predict,[3,4,12] the helical fraction at a fixed temperature is larger for a larger molecular weight. The effect of molecular weight on the transition curve was also examined in two DCA–EDC mixtures differing in DCA content, and we found essentially the same trend as that shown in Figure 3.

Determination of Helix–Coil Transition Parameters s and σ

As is well-established,[3,4,12] the helical fraction of a helix-forming polypeptide in solution can be expressed as a function of the degree of polymerization N of a polypeptide, the equilibrium constant for helix formation s, and the cooperativity parameter σ. Strictly speaking, it may be the average number of intact hydrogen bonds relative to N that can be obtained from ORD or CD measurements,[4] and here we express this quantity by f_N. In order to evaluate the parameter s and σ as functions of temperature and solvent composition, it is convenient to use an approximate expression for f_N derived by Okita, *et al.*[13] under the conditions that $N \gg 1$, $\sigma^{1/2} \ll 1$, and $N\sigma^{1/2} > 2$. For a polydisperse sample, this expression may be written,[4]

$$f_N = f - 2f[f(1-f)]^{1/2}/\bar{N}_n\sigma^{1/2} \quad (1)$$

where f is the value of f_N for infinitely large N related to s and σ by a combined parameter $z = (\ln s)/(2\sigma^{1/2})$:

$$f = (1/2)[1 + z(1+z^2)^{-1/2}] \quad (2)$$

$\bar{N}_n$ is the number-average degree of polymerization of the sample.

Equation 1 holds only when the restricting conditions are satisfied with all the molecular species in the sample. In general, the expression for a polydisperse sample may be written,[4]

$$f_N = \int_0^\infty (f_N)_{\text{mono}} w(N) \mathrm{d}N \quad (3)$$

where $(f_N)_{mono}$ is the helical fraction for a monodisperse sample with N degree of polymerization and $w(N)$ is the weight distribution of N.

As seen in Table I, the samples used for the ORD measurements are polydisperse in molecular weight. Assuming that the samples have molecular weight distributions of the Schulz–Zimm type distribution characterized by their M_w/M_n values, we tried to correct f_N for the polydispersity effect in the following way. First, the experimental f_N under the given solvent conditions is fitted to eq 1 to determine the approximate values of f and σ utilizing the data for samples with large $\bar{N}_n$, and then z is calculated from this f by eq 2; s is obtained from z and σ. Then, with s and σ serving as a guide, f_N is calculated by eq 3 as a function of $\bar{N}_n$ with the polydispersity index M_w/M_n as a parameter for various sets of s and σ, using Nagai's equation for $(f_N)_{mono}$.[14] Figure 4 compares the theoretical f_N thus calculated with the experimental f_N for PCLB in a DCA–EDC mixture containing 55 vol% DCA at 40°C. At large $\bar{N}_n$ for which eq 1 holds approximately, the calculated f_N does not depend on $\bar{N}_w/\bar{N}_n$ but it becomes progressively dependent on $\bar{N}_w/\bar{N}_n$ as $\bar{N}_n$ becomes smaller. However, it is possible to find out from this figure a set of s and σ values which give the best agreement between theory and experiment for possible values of $\bar{N}_w/\bar{N}_n$ (1.3—1.85): $s=1.0047$ and $\sigma^{1/2}=0.0055$. Neglect of the polydispersity effect yielded a slightly larger $\sigma^{1/2}$ (0.006) but essentially the same s. By a similar trial and error method, we

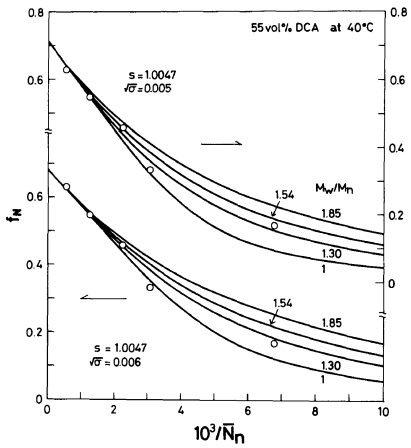

Figure 4. Plots of f_N *vs.* $1/\bar{N}_n$ in the DCA–EDC (55 vol% DCA) mixture at 40°C. Circles denote the experimental data and the solid curves represent the theoretical values calculated for the indicated M_w/M_n. The most probable distribution is used for $w(N)$.

obtained values of s and $\sigma^{1/2}$ for other temperatures in the same solvent mixture, taking $\bar{N}_w/\bar{N}_n$ to be 1.3; the uncertainty in $\sigma^{1/2}$ associated with the curvefitting was ± 0.0005. Figure 5 shows the results from the analysis of the data for the 55 vol% DCA mixture, where the circles denote the experimental data and each solid curve represents the theoretical values calculated for a pair of s and σ giving the best fit to the data points at that temperature. The agreement between theory and experiment is only moderate. Slightly different results were obtained by

Table I. Molecular characterization of Poly(N^{γ}-carbobenzoxy-L-α,γ-diaminobutyric acid)

Sample code	Light scattering[a]			Osmotic pressure[b]			Viscosity,[c] $[\eta]$
	$M_w \times 10^{-4}$	$A_2' \times 10^4$ / cm³ mol g⁻²	$\langle S^2 \rangle^{1/2}$ / Å	$M_n \times 10^{-4}$	$A_2 \times 10^4$ / cm³ mol g⁻²	M_w/M_n	dl g⁻¹
T-1	$67_{.2}$	1.4	77_1	—	—	—	7.95
T-2	$47_{.4}$	2.7	61_7	—	—	—	5.45
T-3	$27_{.0}$	2.3	43_7	18.7	2.9	1.4_4	3.07
T-4	$24_{.2}$	3.0	37_8	$13_{.1}$	3.1	1.8_5	1.90
T-5	$15_{.9}$	2.2	26_7	$10_{.5}$	3.4	1.5_1	1.38
T-6	$10_{.4}$	3.0	17_4	7.6_5	4.5	1.3_6	0.716
T-7	—	—	—	3.4_7	9.4	(1.5)[d]	(0.3)

[a] Measured in dimethylsulfoxide at 25°C.
[b] Measured in *m*-cresol at 70°C.
[c] Measured in dimethylsulfoxide at 25°C.
[d] Rough estimate on the basis of $[\eta]$ in *m*-cresol.

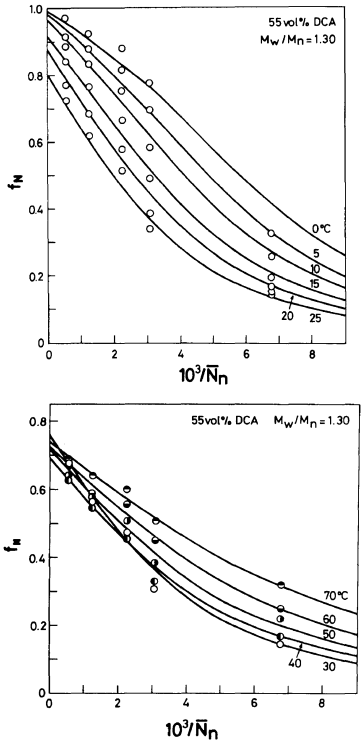

Figure 5. Plots of f_N *vs.* $1/\bar{N}_n$ in the DCA–EDC (55 vol% DCA) mixture at the indicated temperatures. Circles denote the experimental data and solid curves represent the theoretical values calculated for s and $\sigma^{1/2}$ given in Table II. The Schulz–Zimm distribution with $M_w/M_n = 1.3$ is assumed for $w(N)$.

Table II. Helix–coil transition parameters of PCLB in a DCA–EDC (55 vol% DCA) mixture

Temperature/°C	s	$\sigma^{1/2}$
0.0	1.033	0.0025
5.0	1.024	0.0030
10.0	1.018	0.0035
15.0	1.013	0.0040
20.0	1.009	0.0040
25.0	1.007	0.0040
30.0	1.0055	0.0045
40.0	1.0047	0.0055
50.0	1.006	0.0060
60.0	1.0075	0.0072
70.0	1.010	0.009

taking $\bar{N}_w/\bar{N}_n$ to be 1.5, but the data were not accurate enough to detect such a difference. Table II summarizes the numerical results. Similar analyses were performed also with the data for DCA–EDC mixtures containing 56 and 57 vol% DCA, respectively. The type of $w(N)$ was found to have no serious effect on the calculated results. Indeed, an analysis in terms of the logarithmic normal distribution gave essentially the same results as those obtained by the Schulz–Zimm distribution.

The values of s obtained above as a function of the temperature T are plotted against $1/T$ in Figure 6. The data points for each solvent composition follow a curve convex downward, and the curve shifts downward as the DCA content is increased. The latter feature implies that the helical conformation becomes less stable with increasing DCA content. These data can be used to calculate the enthalpy change ΔH accompanying the helix–coil transition by the relation:

$$\Delta H = -R\partial(\ln s)/\partial(1/T) \qquad (4)$$

where R is the gas constant. The values of ΔH calculated by graphical differentiation are shown in Figure 7. These values are about $-170 \sim -150$ cal mol^{-1} at 10°C, zero between 30 and 40°C, and $30 \sim 50$ cal mol^{-1} at 55°C. Gaskin and Yang[5] reported a ΔH of -180 cal mol^{-1} for a normal transition of PCLB in a DCA–chloroform mixture at 5.4°C, whereas Giacometti *et al.*[11] obtained a somewhat larger value of -300 cal mol^{-1} from heat-of-solution measurements on the system PCLB–DCA–EDC. These values may be compared with our

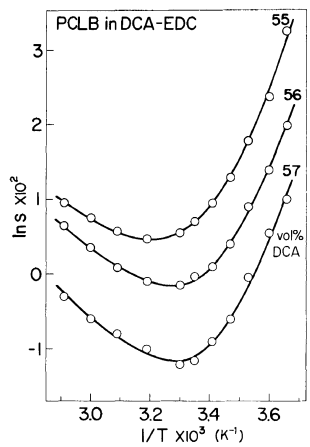

Figure 6. van't Hoff plots of s for PCLB in DCA–EDC mixtures of indicated DCA content.

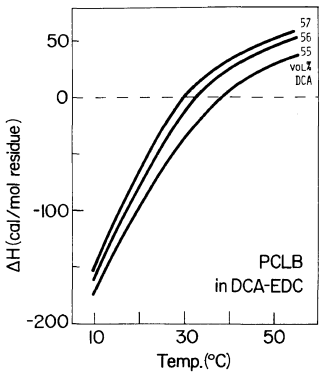

Figure 7. Temperature dependence of transition enthalpy ΔH for PCLB in DCA–EDC mixtures of indicated DCA content.

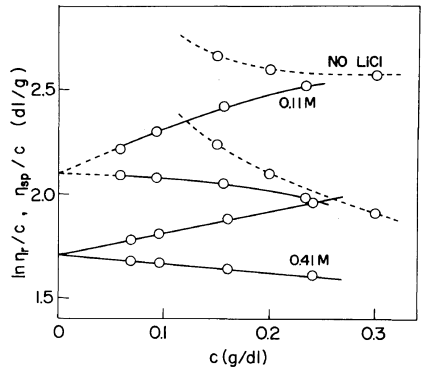

Figure 8. Viscosity data for sample T-2 in DCA containing LiCl of the indicated molarities at 25°.

result that ΔH is about -200 cal mol^{-1} at lower temperatures.

As mentioned in the introduction, the helix stability of a helix-forming polypeptide in a mixture of a helix-supporting solvent and helix-breaking solvent is determined by two competitive actions: a helix formation by intramolecular hydrogen bonding, and solvation of the backbone amide groups by helix-breaking solvent. In a solvent mixture of appropriate composition, the polypeptide is expected to undergo an inverse thermal transition at lower temperatures and a normal transition at higher temperature.[4,6,15,17] This prediction does not hold for PCLB in DCA–EDC, in which a normal transition is followed by an inverse transition with raising temperature. Hatano and Yoneyama[16] found from ORD measurements that among its homologs PCLB has the most stable helical conformation in DCA–$CHCl_3$. According to these authors, the helical conformation is stabilized by intramolecular hydrogen bonds between the nearest neighboring urethane linkages on the side chains; the fraction of bonded urethane linkages is largest for PCLB. If we assume that this hydrogen bond fraction decreases appreciably with raising temperature, we can explain the dual thermal transition of PCLB by incorporating the side-chain hydrogen bonding into the solvation mechanism of Sayama, *et al.*[17] We made IR measurements on PCLB in $CHCl_3$, which revealed, in agreement with Hatano and Yoneyama, two NH stretching bands: a free NH band at 3450 cm^{-1} and a hydrogen-bonded NH band at 3300 cm^{-1}. However, the changes in intensity of the two bands with temperature were not appreciable enough to substantiate the above explanation.

We attempted to use viscosity measurements to examine the change in the average dimensions of PCLB molecules accompanying the dual transition. However, when pure DCA or mixtures of DCA and EDC were used as solvents, this attempt was hampered by a pronounced polyelectrolytic effect. Figure 8 shows typical viscosity data for DCA solutions; for pure DCA, η_{sp}/c increases as the polymer concentration c is decreased, but this upswing in η_{sp}/c disappears if a small amount of LiCl is added. Thus, PCLB in DCA shows typical polyelectrolytic behavior.

Figure 9 shows plots of b_0 *vs.* temperature for PCLB in DCA–EDC mixtures (56 vol% DCA) containing various amounts of LiCl. It can be seen that only a trace of LiCl changes drastically the transition behavior at lower temperatures. A concentration of LiCl as small as 0.021 mol l^{-1} is almost sufficient to suppress the helix formation over the range of temperature studied. This change in the transition curve is opposite to what would be expected from the usual solvation mechanism,[4,6,17] since LiCl is considered to suppress the helix-breaking action of DCA and thus to promote the helix formation. We believe that the polyelectrolytic behavior of PCLB in DCA–EDC is, at least in part, responsible for the dual thermal transition, although no detailed mechanism has been elucidated as yet.

The temperature dependence of $\sigma^{1/2}$, shown in Figure 10, indicates that $\ln \sigma^{1/2}$ for a given solvent mixture varies linearly with $1/T$. The lines for the

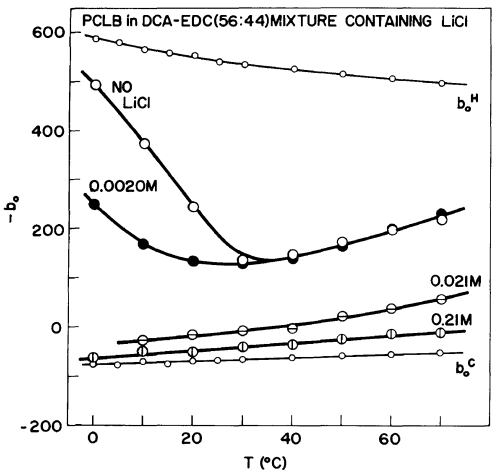

Figure 9. Temperature dependence of Moffitt parameter b_0 for sample T-2 in DCA–EDC (56 vol% DCA) mixtures containing LiCl. The LiCl content is expressed in molarity.

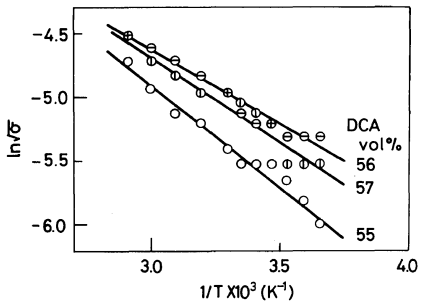

Figure 10. vat't Hoff plots of $\sigma^{1/2}$ for PCLB in DCA–EDC mixtures of indicated DCA content.

three mixtures have nearly the same slopes and give *ca.* 5.6 kcal mol^{-1} for the enthalpic component of σ, ΔH_σ. It is noted that this value of ΔH_σ is close to the theoretical value predicted for polyalanine in water by Go *et al.*[18]

Conformation in Helix-supporting Solvents

Figure 11 shows plots of $\langle S^2\rangle^{1/2}$ against the weight-average degree of polymerization, $\bar{N}_w$, for several polypeptides in helix-supporting solvents. Here, the solid line indicates the relation for α-helical straight rods with a pitch per one monomeric residue of 1.5 Å. The data points for PCLB deviate downward systematically from the straight line as

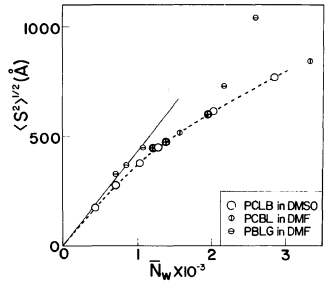

Figure 11. Plots of root-mean-square radius of gyration $\langle S^2\rangle^{1/2}$ *vs.* weight-average degree of polymerization $\bar{N}_w$ in helix-supporting solvents: (○), the present data for PCLB in DMSO at 25°C; (⊕), PCLO in DMF at 25°C;[20] (⊙), PCBL in DMF at 25°C;[19] (⊖), PBLG in DMF at 25°C.[21]

the molecular weight is increased. Thus we find that PCLB in DMSO assumes the α-helical rod at relatively low molecular weights, but becomes increasingly flexible with an increase in molecular weight. Behavior similar to this has been noted in other polypeptides,[3] as is illustrated in Figure 11 with data for typical polypeptides. In terms of these data for mean-square radius of gyration, we may conclude that PCLB in DMSO is nearly as flexible as PCBL in DMF[19] and PCLO in DMF,[20] and these are more flexible than PBLG in DMF.[21]

The molecular conformation of PCLB in DMSO may be visualized as an α-helical rod containing random coil portions. This picture is an interrupted helix. Nagai[14] has given an expression for $\langle S^2\rangle$ of an interrupted helix as a function of s, σ, a_0, and a_1, where a_0 is the effective bond length of the random coil and a_1 is the pitch per monomeric residue of helical rod. We used his expression to calculate $\langle S^2\rangle$ for various combinations of s and σ, with $a_0 = 15$ Å and $a_1 = 1.5$ Å.[3,21] The calculated $\langle S^2\rangle$ (thick solid curve) are compared with experimental data (circles) in Figure 12. It is seen that a combination of $s = 1.5$ and $\sigma^{1/2} = 0.03$ enables the theory to agree with the experimental results. However, since many other combinations of s and $\sigma^{1/2}$ give equally good fits to the experimental data, the light scattering data are not enough to decide on the best combination of s and $\sigma^{1/2}$.

The molecular conformation of PCLB in DMSO may also be approximated by a broken rod consisting of helical rods connected by short random coil portions. Nagai's theory gives the average number of helical rods in a polypeptide chain as a

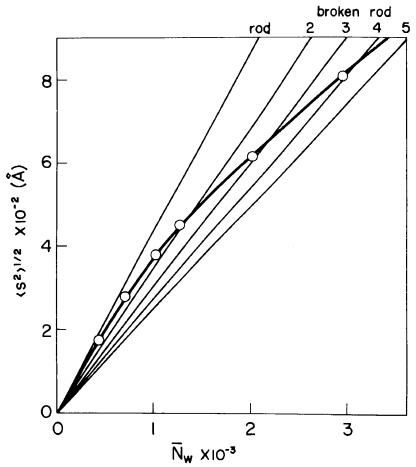

Figure 12. Dependence of root-mean-square radius of gyration on degree of polymerization. The circles are the data for PCLB in DMSO at 25°C. The thick line denotes the theoretical values calculated by Nagai's theory with $s=1.5$ and $\sigma^{1/2}=0.030$, and the thin straight lines represent the values for a straight rod and broken rods,[22,23] with the pitch per monomeric residue taken to be 1.5 Å. The figures attached to the lines denote the number n of rods per one chain.

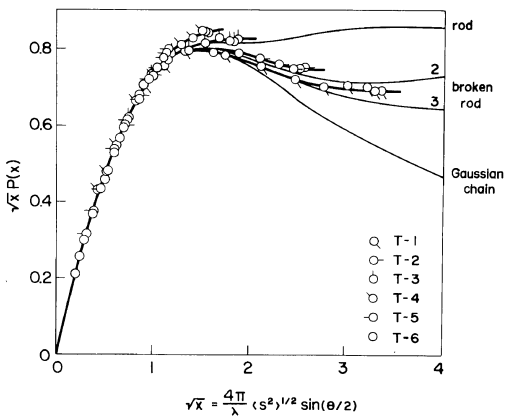

Figure 13. Plots of $x^{1/2}\,P(x)$ *vs.* x. $x=(4\pi/\lambda)^2\langle S^2\rangle\sin^2(\theta/2)$ and the z-average mean-square radius of gyration is used for $\langle S^2\rangle$ to plot the experimental data. The thin lines represent the theoretical values for a straight rod, broken rods, and a Gaussian chain.

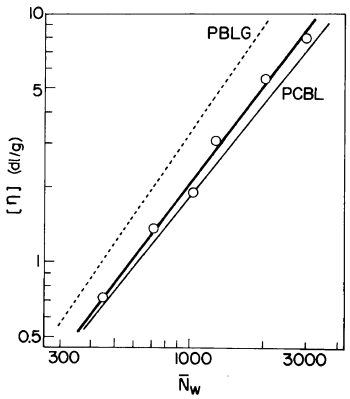

Figure 14. Plots of $[\eta]$ *vs.* $\bar{N}_w$ in helix-supporting solvents at 25°C. The circles are the experimental data for PCLB in DMSO at 25°C, and the thin solid and broken lines denote the experimental values for PCBL[19] and PBLG[25] in DMF, respectively.

function of s and σ. With $s=1.5$ and $\sigma^{1/2}=0.03$, the number is estimated to be 2.0 for $N=444$, 2.6 for $N=679$, 3.4 for $N=1034$, 4.0 for $N=1154$, 5.7 for $N=2017$, and 7.6 for $N=2872$. Essentially the same results were obtained with other combinations of s and $\sigma^{1/2}$ which had been used for calculating $\langle S^2\rangle$. The thin straight lines in Figure 12 represent $\langle S^2\rangle^{1/2}$ for broken rods consisting of n rods of equal length, calculated according to Hermans and Hermans.[22] The experimental data are consistent with the broken rod model provided n is equal to about half the average number of helical rods estimated by Nagai's theory. This difference can be ascribed to the fact that the lengths of the helical rods are equal to each other in the broken rod model, but are statistically distributed in the interrupted helix model.

Figure 13 compares the experimental particle scattering function $P(x)$ with the theoretical values calculated for various molecular models including the broken rod.[22,23] Here x is $(4\pi/\lambda)^2\langle S^2\rangle\sin^2(\theta/2)$, θ is the scattering angle, and λ is the wavelength of incident light in the scattering medium. For values of x smaller than unity, the experimental data for any fraction follow a single theoretical curve common to all the models examined, thus giving no information about the molecular conformation. The data points for fractions T-3 and T-4 level off at x values larger than unity; and this fact suggests that the molecular shapes be rodlike. On the other hand, neither the straight rod nor the Gaussian chain appears to be compatible with the data for the two high-molecular-weight fractions T-1 and T-2, which tend to exhibit the features of a broken rod. Thus, the shape of scattering function is consistent with the above-

mentioned molecular weight dependence of the mean-square radius of gyration. However, the numbers n of rods obtained from $\langle S^2 \rangle$ and $P(x)$ are different; *e.g.*, for the fraction T-1, $n=4$ from $\langle S^2 \rangle$ and $n=2\sim3$ from $P(x)$. Calculations show that the curve of $x^{1/2}P(x)$ for a large x value appreciably varies with the molecular weight distribution of the sample and with the dispersion of the lengths of the helical rods. Both these factors tend to make the value of $x^{1/2}P(x)$ larger than that for a monodisperse sample or a uniform broken rod. Thus, the number of rods obtained from $P(x)$ may be underestimated, since the samples are polydisperse and the distribution of break points on the polypeptide chain may be random.

Intrinsic Viscosity

Figure 14 shows a double-logarithmic plot of $[\eta]$ *vs.* $\bar{N}_w$ for PCLB in DMSO at 25°C. The data points follow a straight line represented by

$$[\eta]=1.67\times10^{-7}\ M_w^{1.32}$$

The exponent 1.32 is lower than the theoretical value 1.7 for long straight rods,[3] but higher than the highest value 0.80 expected for randomly coiled molecules.[24] In the same figure, the data for PCBL in DMF[19] and PBLG in DMF[25] are included for comparison. If compared at the same $\bar{N}_w$, the $[\eta]$ value for PCLB is slightly higher than that of PCBL but considerably lower than that of PBLG; the exponents are 1.27 for PCBL and 1.45 for PBLG. Thus the helical conformation of PCLB in DMSO may be nearly as stable as that of PCBL in DMF, but the helices of these polypeptides are less stable than that of PBLG in DMF, as has also been inferred from the $\langle S^2 \rangle$ values. Table I contains intrinsic viscosities of PCLB fractions in DMSO at 25°C. Almost the same values were obtained in *m*-cresol at 25°C.

Acknowledgments. The authors wish to thank Professor Hiroshi Fujita for his valuable comments.

REFERENCES

1. P. Urnes and P. Doty, *Adv. Protein Chem.*, **16**, 401 (1961).
2. G. D. Fasman, in "Poly-α-Amino Acids," G. D. Fasman, Ed., Marcel Dekker, New York, N.Y., 1967, Chapter 11.
3. A. Teramoto and H. Fujita, *Adv. Polym. Sci.*, **18**, 65 (1975).
4. A. Teramoto and H. Fujita, *J. Macromol. Sci., Rev. Macromol. Chem.*, **C15**, 165 (1976).
5. F. Gaskin and J. T. Yang, *Biopolymers*, **10**, 631 (1971).
6. F. E. Karasz and G. G. Gajnos, *J. Phys. Chem.*, **77**, 1139 (1973).
7. D. W. Adamson, *J. Chem. Soc.*, 1564 (1939).
8. M. J. Fridecky and W. H. McGregor, *J. Med. Chem.*, **9**, 255 (1966).
9. Y. Miyaki, Y. Einaga, T. Hirosye, and H. Fujita, *Macromolecules*, **10**, 1356 (1977).
10. "Organic Solvents," A. Weissberger, E. S. Proskauer, J. A. Riddick, and E. E. Toops, Jr., Ed., Interscience Publishers, New York, N.Y., 1955.
11. G. Giacometti and A. Turolla, *Biopolymers*, **11**, 215 (1972).
12. D. Poland and H. A. Scheraga, "Theory of Helix–Coil Transitions in Biopolymers," Academic Press, New York, N.Y., 1970.
13. K. Okita, A. Teramoto, and H. Fujita, *Biopolymers*, **9**, 717 (1970).
14. K. Nagai, *J. Chem. Phys.*, **34**, 887 (1961).
15. R. P. McKnight and F. E. Karasz, *Macromolecules*, **7**, 143 (1974).
16. M. Hatano and M. Yoneyama, *J. Am. Chem. Soc.*, **92**, 1392 (1974).
17. N. Sayama, K. Kida, T. Norisuye, A. Teramoto, and H. Fujita, *Polym. J.*, **3**, 538 (1971).
18. M. Go, N. Go, and H. A. Scheraga, *J. Chem. Phys.*, **54**, 4489 (1971).
19. M. Matsuoka, T. Norisuye, A. Teramoto, and H. Fujita, *Biopolymers*, **12**, 1515 (1973).
20. H. Mishima and A. Teramoto, unpublished data.
21. T. Norisuye, A. Teramoto, and H. Fujita, *Polym. J.*, **3**, 323 (1973).
22. J. Hermans and J. J. Hermans, *J. Phys. Chem.*, **62**, 1543 (1958).
23. P. Kratochvil, in "Light Scattering from Polymer Solutions," M. B. Huglin, Ed., Academic Press, New York, N.Y., 1971.
24. H. Yamakawa, "Modern Theory of Polymer Solutions," Harper & Row, New York, N.Y., 1971.
25. T. Norisuye, Ph. Doctral Thesis, Osaka University, 1973.